Investigation of Hardening Effects on the Dynamics of structure by using electromagnetic actuator

Lei ZENG *, Jin ZHOU * Jarir MAHFOUD**, Yuanping Xu*, and Chaowu JIN*
* College of Mechanical & Electrical Engineering, Nanjing University of Aeronautics and Astronautics
No. 29, Yudao Street, Nanjing, Jiangsu 210016, China
E-mail: zhj@nuaa.edu.cn
** INSA-Lyon, CNRS-UMR5259, LaMCoS
INSA-Lyon, F-69621 Villeurbanne Cedex, France

Abstract
The effect of an electromagnetic actuator (EMA) with an LCR circuit on the frequency response of a cantilever beam is investigated in this paper using theoretical analysis and numerical simulation. Specifically, the effects of the influent parameters, such as the air gap of EMA and the amplitude and frequency of the LCR circuit, were assessed regarding their modulation effects on the dynamic behaviour of the system. The aim is to optimize the design of the test rig. The theoretical analysis based on the harmonic balance method is used to solve the electromechanical coupled dynamic equations of the system. The results show that the system can introduce a controlled hardening effect in the structure. Furthermore, it can be seen that the hardening characteristic of the system could be controlled with the variation of the excitation voltage amplitude or the proximity of the driving frequency to the resonance frequency of the circuit. The theoretical analyses are in good agreement with the numerical simulation results. The results obtained provide the required elements for the design of the test rig necessary for the experimental validation.

Keywords: Electromagnetic actuator, LCR circuit, Flexible structure, Hardening effect, Harmonic Balance Method, nonlinear dynamics

1. Introduction

Nonlinearity is a common feature in the dynamics of modern mechanical systems, manifesting in diverse forms (Nayfeh and Mook, 1979; Virgin, 2000). A primary challenge involves suppressing large-amplitude vibrations and effectively mitigating hysteresis within these systems. Hysteresis is a particularly critical factor that can induce dynamic instability, especially in structures featuring localized nonlinearities. This behavior often manifests in the forced vibration response as a jump phenomenon—a sudden and irreversible change in the system's response amplitude as the excitation frequency is varied. However, from a vibration control perspective, these same nonlinearities can be strategically exploited to modulate system dynamics, typically through hardening or softening effects that alter the resonant behavior.

Electromagnetic actuators (EMAs) are widely used in various industrial applications as a simple and reliable non-contact excitation source. However, the electromagnetic force they generate is inherently nonlinear — proportional to the square of the coil current and inversely proportional to the square of the air gap —a characteristic that significantly influences the system's dynamic behavior. Under constant current control, EMAs introduce a softening nonlinear characteristic to the system (Belhaq et al., 2011). This softening effect shifts the structure's resonant frequency to a lower value, causing it to fall within the equipment's normal operating range and induce highly detrimental resonance. Therefore, effectively utilizing the EMA's inherent nonlinearity to achieve desired modulation of the system's dynamic characteristics has become a key scientific challenge.

Tuned LC circuits have been demonstrated to provide a stable equivalent stiffness near the resonant frequency (Higuchi and Jin, 1992). For instance, Chen et al. (2008) designed a magnetic levitation bearing for a heart pump, incorporating tuned LCR circuits to stabilize the rotor's central position without active control. Similarly, Kimura and Sugiura (2024) utilized parallel LCR circuits as dampers to achieve effective vibration suppression. Investigating the dynamic characteristics of a cantilever beam under high-frequency electromagnetic excitation, Bichri et al. (2014) demonstrated that the first bending mode could be shifted to either lower or higher frequency by adjusting the amplitude of the current supplied to the EMA. These findings suggest that combining the LCR circuit with EMAs offers a method for tuning the system's effective stiffness, enabling the transition between softening and hardening effects to actively mitigate potential resonance.

The purpose of this paper is to systematically investigate the mechanism of EMAs with LCR circuits on structural dynamics by combining theoretical analysis and numerical simulation. This study will focus on analysing the influence of key parameters such as voltage source voltage, voltage source frequency, and air gap of the EMA on the nonlinear stiffness of the system, which will provide theoretical guidance to optimize the design of the test rig that will be dedicated to subsequent experimental studies.

2. Modelling of the system

2.1 Description of the test rig

The system consists of a cantilever beam with a rectangular cross-section (350 mm length × 26 mm width × 3 mm height), clamped at one end and fitted with an EMA at the free end (Fig. 1(a)). An excitation point and a response measurement point are located 100 mm and 180 mm from the fixed end, respectively. The EMA is mounted 250 mm from the clamped end, a position selected to effectively excite the first three structural modes. The EMA is composed of an E-type core, integrated with the coil, and an I-type armature affixed to the cantilever beam. The specific dimensions of EMA are shown in Fig. 1(b). Since a single EMA can generate only unidirectional attraction, this study utilizes a pair of identical, independently controlled actuators. As depicted in Fig. 2, the coil (providing inductance L) of each actuator is connected in series with a capacitor (C) and a resistor (R) to form an LCR circuit. The dimensions of the different components of this test rig were chosen to have a suitable frequency range and sufficient electromagnetic force. The dynamic equation of the system is as follows.

$$m\ddot{x} + c\dot{x} + kx = F_{ex} + F_{em} \tag{1}$$

Where m is the mass, c is the damping, k is the stiffness, Fem is the electromagnetic force, and F_{ex} is the external harmonic excitation with amplitude A_0 and frequency ω_e.

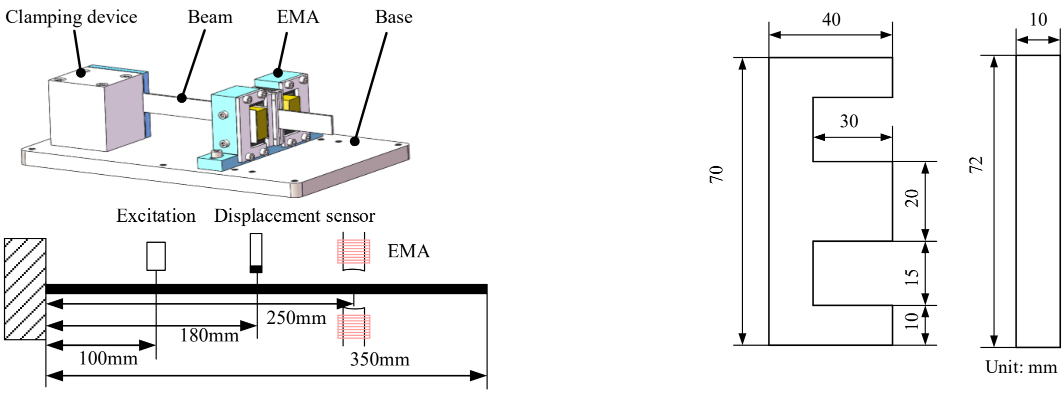

Fig. 1 (a) Test rig. (b) EMA specific dimension

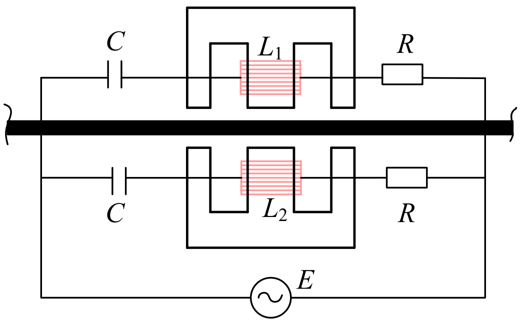

Fig. 2 The EMA is connected to the LCR circuit

2.2 Electromagnetic force modelling

Applying magnetic circuit theory, and assuming that the effects of eddy currents and magnetic flux leakage are negligible, the relationship between the electromagnetic force (F_{em}), air gap (e), beam displacement (x), and coil current is expressed as(Bichri et al.,2014):

$$F_{em} = \frac{N^2 \mu_0 A I_1^2}{(e - x + \frac{b+c+d-2a}{\mu_r})^2} - \frac{N^2 \mu_0 A I_2^2}{(e + x + \frac{b+c+d-2a}{\mu_r})^2} \tag{2}$$

Where a,b,c,d are the structural parameters of the EMA, μ_0 is the air permeability, μ_r is the relative permeability of the core material, N is the number of turns of the coil, A is the cross-section area of the magnetic poles, I_1 and I_2 are the currents in the two coils, respectively.

2.3 LCR circuit

The integration of the LCR circuit with the EMA facilitates a passive control strategy, enabling both self-sensing and inherent positional stability. Applying Kirchhoff's voltage law, the governing equation for the electrical dynamics of the circuit is given by:

$$\frac{1}{C}\frac{dq}{dt} + R\frac{di}{dt} + L\frac{d^2 i}{dt^2} = \frac{dE}{dt} \tag{3}$$

Where: q is the electric quantity and i is the current.

For a constant source voltage, differentiating the preceding first-order equation concerning time and dividing by the inductance (L) yields the following second-order differential equation:

$$\frac{d^2 i}{dt^2} + \frac{R}{L}\frac{di}{dt} + \frac{1}{CL} i = \frac{1}{L}\frac{dE}{dt} \tag{4}$$

The LCR circuit is driven by a sinusoidal voltage source operating at a fixed frequency, which is intentionally set slightly above the circuit's resonant frequency. The resonant frequency of the LCR circuit can be written as：

$$f_{cir} = \frac{1}{2\pi\sqrt{LC}} \tag{5}$$

The operational principle of the EMA-LCR system involves leveraging the resonant characteristics of the circuit to modulate the coil current, which in turn alters the equivalent stiffness generated by the electromagnetic force. The system's ability to exhibit a hardening effect is critically dependent on how variations in the EMA's inductance—caused by beam displacement—shift the circuit's operating point relative to its resonance. To ensure that inductance variations have a dominant effect on the circuit's dynamics, a relatively small capacitance value must be selected. Accordingly, a capacitance of 0.1 μF is used in this investigation. The inductance of the EMA is a function of both the air gap and beam displacement, and this relationship is expressed as follows:

$$L = \frac{N^2 \mu_0 A}{2\left(e - x + \frac{L_s}{\mu_r}\right)} \tag{6}$$

Where L_s is the coil length

Figure 3 illustrates the calculated resonant frequency range of the LCR circuit for a representative beam vibration amplitude of x = 0.15 mm. Accordingly, to investigate the system's hardening characteristics, the supply voltage frequency is set to a value slightly above the upper bound of this calculated resonant range for all subsequent analyses.

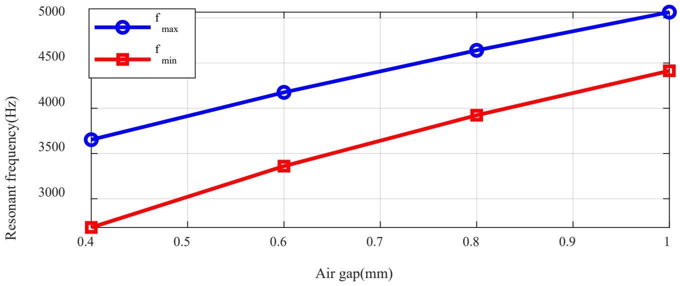

Fig. 3 Variation range of resonant frequency of LCR circuit.

3. Theoretical analysis of the non-linear characteristics of the system

3.1 Static analysis of electromagnetic forces

Under steady-state sinusoidal voltage excitation, the current in the LCR circuit can be expressed as:

$$I = \frac{V^2}{\sqrt{R^2 + (\omega L - \frac{1}{\omega C})^2}} \tag{7}$$

Where V is the voltage source amplitude and ω is the voltage source excitation frequency

Substituting Eqs. (6)and (7) into Eq. (2) yields the following expression for the electromagnetic force:

$$F_{em}(x) = \frac{\dfrac{N^2\mu_0 A V^2}{R^2 + (\omega \dfrac{N^2\mu_0 A}{2\left(e - x + \dfrac{L_s}{\mu_r}\right)} - \dfrac{1}{\omega C})^2}}{(e - x + \dfrac{b+c+d-2a}{\mu_r})^2} - \frac{\dfrac{N^2\mu_0 A V^2}{R^2 + (\omega \dfrac{N^2\mu_0 A}{2\left(e + x + \dfrac{L_s}{\mu_r}\right)} - \dfrac{1}{\omega C})^2}}{(e + x + \dfrac{b+c+d-2a}{\mu_r})^2} \tag{8}$$

The complex form of the right-hand side of Eq. (8) renders direct analysis intractable; therefore, a Taylor series expansion is employed to derive a more tractable, approximate expression for the electromagnetic force.

$$k_1 = \frac{dF_{em}}{dx}\Big|_{x=0}, k_2 = \frac{1}{2}\frac{d^2 F_{em}}{dx^2}\Big|_{x=0}, k_3 = \frac{1}{6}\frac{d^3 F_{em}}{dx^3}\Big|_{x=0} \tag{9}$$

Since $F_{em}(x)$ is an odd function, according to the properties of a Taylor series, the expansion of an odd function about the origin (x=0) contains only odd-power terms, which means the coefficient of the second-order term, k_2, must be zero. The system dynamics equation can be written as

$$m\ddot{x} + c\dot{x} + (k + k_1)x + k_3 x^3 = A_0 \sin\omega_e t \tag{10}$$

To solve the nonlinear dynamics equation(10), this paper employs the harmonic balance method and assumes that the first harmonic solution of the system has the following form.

$$x(t) = A_1 \sin\left(\omega_e t + \phi\right) \tag{11}$$

Bringing in the equation(10), there is

$$-mA_1\omega_e^2 \sin\left(\omega_e t + \phi\right) + cA_1\omega_e \cos\left(\omega_e t + \phi\right) + (k + k_1)A_1 \sin\left(\omega_e t + \phi\right) + \frac{3}{4}k_3 A_1^3 \sin\left(\omega_e t + \phi\right) = A_0 \sin\left(\omega_e t\right) \tag{12}$$

Combining the sin($\omega_e t$) and cos($\omega_e t$) like harmonic terms on both sides of the equation yields

$$\begin{cases} A_1\ [(k + k_1\ -\ m\omega_e^2 + \frac{3}{4}k_3 A_1^2) cos\phi - c\omega_e \sin\phi] \sin\omega_e t = A_0 \sin\omega_e t \\ A_1\ [(k + k_1\ -\ m\omega_e^2 + \frac{3}{4}k_3 A_1^2) \sin\phi + c\omega_e \cos\phi] \cos\omega_e t = 0 \end{cases} \tag{13}$$

The amplitude-frequency response equation of the system can be written as an equation(14).

$$\left(\left(k + k_1\right) - m\omega_e + \frac{3}{4}k_3 A_1^2\right)^2 + \left(c\omega_e\right)^2 = \left(\frac{A_0}{A_1}\right)^2 \tag{14}$$

3.2 Analysis of parameter effects

The nonlinear hardening characteristics of the integrated EMA-LCR system are governed by three key parameters: the EMA air gap, the amplitude and frequency of the voltage. The nominal values for the key EMA and LCR circuit parameters used throughout this investigation are listed in Table 1. This analysis is done for the chosen structure geometrie and EMA.

Table 1 Parameters of EMA and LCR circuit

parameter	symbol	value	parameter	symbol	value
Width of the pole(mm)	a	10	Capacitance(F)	C	1×10^{-7}
Width of E-type(mm)	b	40	Resistance(Ω)	R	1
Half length of E-type(mm)	c	35	1st frequency (rad/s)	ω_n	$11.6\times2\pi$
Width of I-type(mm)	d	10	Stiffness (N/m)	k_1	1.7×10^6
Coil turns	N	270	Damping coefficient(Ns/m)	c	9.3
Area of the pole(mm^2)	A	270	Amplitude of excitation(N)	A_0	0.1

3.2.1 Effect of Air Gap

To investigate the influence of the air gap on system response, amplitude-dimensionless frequency response curves were computed for various air gaps using a fixed voltage of 15 V, as plotted in Fig. 4(a). The figure reveals that reducing the air gap significantly enhances the system's nonlinear hardening effect. This behavior is attributed to the fact that a smaller air gap increases both the electromagnetic force and its gradient with respect to displacement (i.e., the equivalent linear stiffness k_1 and nonlinear stiffness k_3), thereby amplifying the hardening effect. Furthermore, the parameter scan results in Fig. 4(b) indicate that the hardening effect is most prominent when combining a small air gap with a high supply voltage, achieving a maximum resonant frequency shift of up to 2.1.

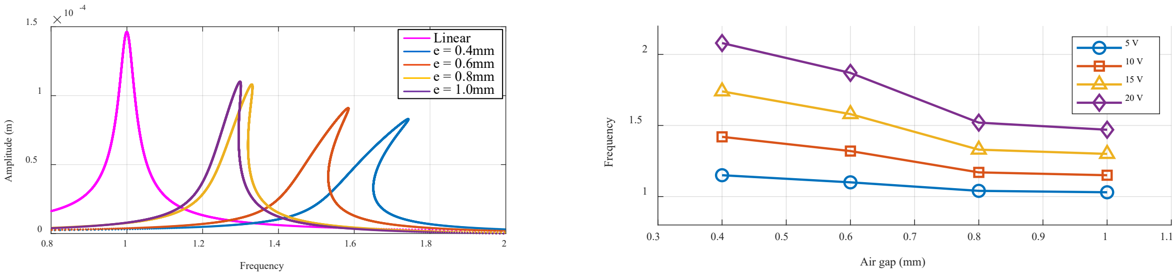

Fig. 4 (a)Effect of air gap on the system response, (b) Effect of air gap and voltage on the system response

3.2.2 Effect of Voltage Source Amplitude

Figure 5 illustrates the influence of the supply voltage on the system response, with the air gap and source frequency held constant at 0.8 mm and 4900 Hz, respectively. Increasing the supply voltage accentuates the system's nonlinear hardening characteristic, which is evidenced by a shift in the dimensionless resonant frequency from 1.0 to 1.5 and a concurrent, significant suppression of the beam's peak resonant amplitude. This is because higher voltage induces a larger current in the LCR circuit, which increases the magnitude of the electromagnetic force, thereby strengthening the nonlinear stiffness and enhancing the vibration suppression effect.

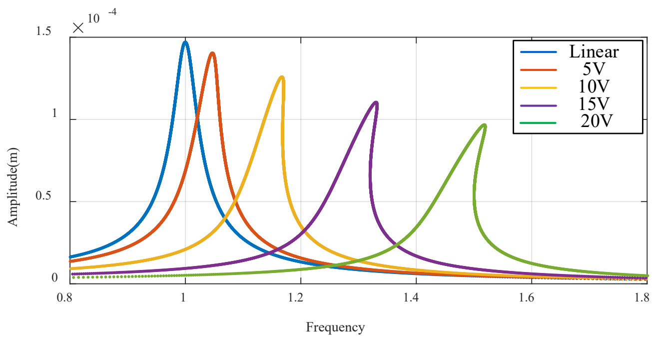

Fig. 5 Effect of voltage amplitude on the system response

3.2.3 Effect of Voltage Source Frequency

The LCR circuit is excited by a voltage source of fixed frequency; the excitation frequency of the voltage source should be greater than the resonance frequency of the circuit, because when the frequency of the voltage source is chosen too close to the resonance frequency of the circuit, it will lead to resonance of the circuit. Figure 6 presents the calculated system response for a fixed air gap of 0.8 mm and voltage of 15 V, while varying the source frequency. The results show that, for a constant voltage, the hardening characteristic becomes more pronounced as the source frequency is decreased towards the circuit's resonant frequency from above. This occurs because approaching the resonant frequency from the high-frequency side reduces the total impedance of the LCR circuit, leading to an increased coil current and, consequently, a stronger electromagnetic force that augments the system's nonlinear stiffness.

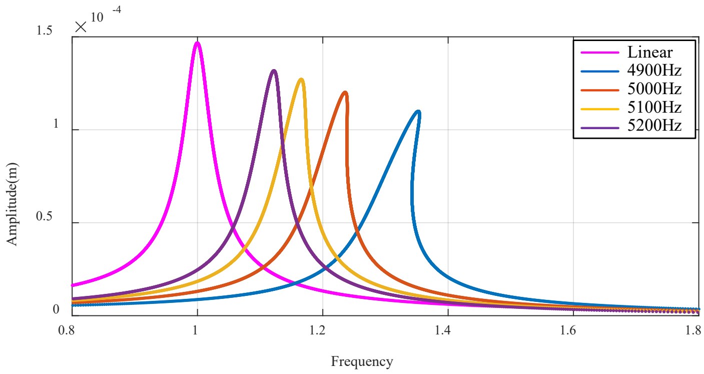

Fig. 6 Effect of voltage frequency on the system response

4. Numerical simulation results

Numerical simulations were conducted to validate the theoretical model and to investigate complex dynamic behaviors potentially omitted by the model's simplifying assumptions. The structural dynamics of the cantilever beam were modeled using the finite element method (FEM). This FEM model comprises 20 beam elements, with each node possessing two degrees of freedom (DOF): translation and rotation. By integrating the FEM structural model with the electrical circuit equations, the complete coupled system is represented by the following state-space equation:

$$\begin{bmatrix} \dot{\mathbf{x}} \\ \ddot{\mathbf{x}} \end{bmatrix} = \begin{bmatrix} \mathbf{0} & \mathbf{I} \\ -\mathbf{M}^{-1}\mathbf{K} & -\mathbf{M}^{-1}\mathbf{C} \end{bmatrix} \begin{bmatrix} \mathbf{x} \\ \dot{\mathbf{x}} \end{bmatrix} + \begin{bmatrix} \mathbf{0} \\ \mathbf{M}^{-1} \end{bmatrix} \left(\mathbf{F}_{ex} + \mathbf{F}_{em} \right) \tag{15}$$

Where **M**, **K**, and **C** are the mass, stiffness, and damping matrices, respectively, and $\boldsymbol{x}$、$\dot{\boldsymbol{x}}$、$\ddot{\boldsymbol{x}}$ are the displacement, velocity, and acceleration, respectively.

Given that vibration energy is primarily concentrated in the lower-order modes and this study focuses on dynamics near the first resonance region, a modal truncation approach was employed to reduce the model's order, thereby improving computational efficiency while maintaining accuracy. For this purpose, the first six modes were retained. The system was excited with a 0.1 N sinusoidal force, applied at the designated excitation node, sweeping linearly from 8 Hz to 25 Hz over a 200 s duration. The initial set of simulations, presented in Fig. 7, was designed to validate the predicted influence of the air gap on the system dynamics. The numerical results align with the theoretical predictions, confirming that reducing the initial air gap significantly amplifies the hardening effect and shifts the dimensionless resonant frequency from 1.0 to 1.65.

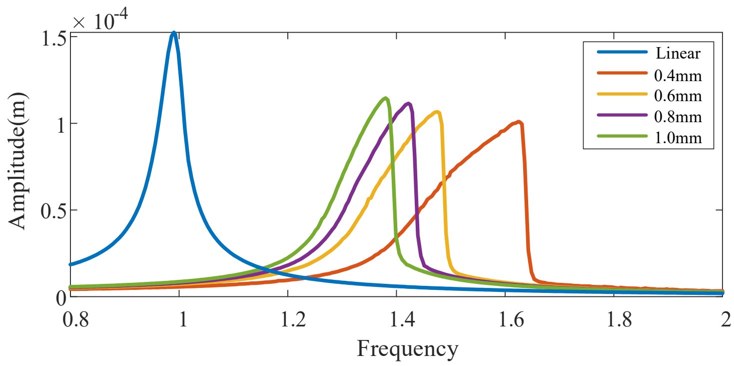

Fig. 7 Effect of air gap on the system response

Furthermore, the investigation examined the influence of voltage amplitude and frequency on the system's response, with the air gap held constant at 0.8 mm. As depicted in Fig. 8(a), for a fixed source frequency, the system continues to exhibit hardening behavior even at reduced supply voltage amplitudes. Similarly, Fig. 8(b) indicates that for a fixed voltage, the system's hardening effect becomes more pronounced as the source frequency approaches the LCR circuit's resonant frequency. These simulation findings show strong qualitative agreement with the theoretical predictions, thereby validating the fidelity of both the analytical and numerical models developed in this study.

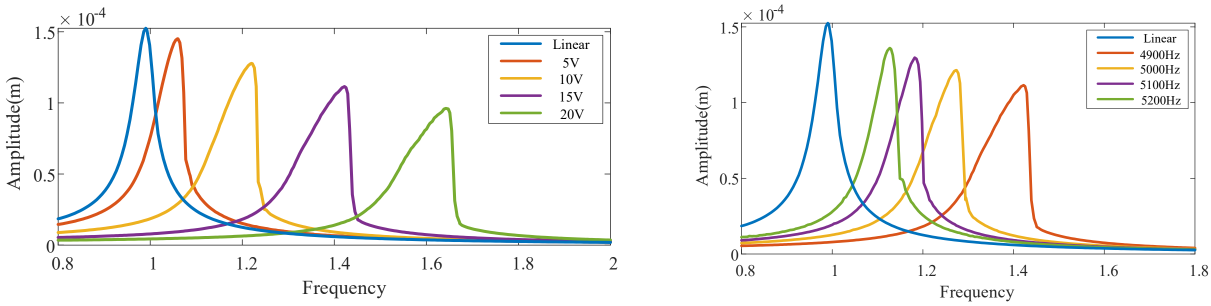

Fig. 8 (a)Effect of voltage amplitude on the system response, (b) Effect of voltage frequency on the system response

5. Conclusion

This paper presented a systematic investigation into the influence of integrated EMA-LCR circuits on the dynamic characteristics of a cantilever beam, utilizing a combined theoretical and numerical approach. A nonlinear analytical model of the electromagnetic force was developed and subsequently solved using the harmonic balance method to predict the system's amplitude-frequency response. The aim is to build up a reliable model for the optimization of structures under variable frequency operating conditions. The results show that the system can introduce a controlled hardening effect in the structure. Furthermore, it can be seen that the hardening characteristic of the system could be controlled with the variation of the excitation voltage amplitude or the proximity of the driving frequency to the resonance frequency of the circuit.

References

Belhaq, M., Bichri, A., Der Hogapian, J., and Mahfoud, J., Effect of electromagnetic actuations on the dynamics of a harmonically excited cantilever beam, International Journal of Non-Linear Mechanics, Vol.46, No.6(2011), pp.828 – 833.

Bichri, A., Belhaq, M., Mahfoud, J., Effect of high-frequency AC electromagnetic actuation on the dynamic of an excited cantilever beam, Proceedings of MATEC Web of Conferences, Vol.16 (2014), Art. No. 08002.

Chen, H. M., Chapman, P. A., Donahue, A. C., et al., A Magnetically Levitated Blood Pump using LCR Circuits, Proceedings of 11th International Symposium on Magnetic Bearings (ISMB) (2008), pp.212-216.

Higuchi, T. and Jin, J., Modeling and dynamic stabilization for suspension system using tuned lc circuit, Proceedings of IEEE International Conference on Systems Engineering (1992), pp.411–415.

Kimura, K. and Sugiura, T., Vibration Modal Analysis of Superconducting Levitation With LCR Shunt Damper, IEEE Transactions on Applied Superconductivity, Vol.34, No.3 (2024), pp.1-4.

Nayfeh, A. H. and Mook, D. T., Nonlinear Oscillations, Wiley, (1979).

Virgin, L. N., Introduction to Experimental Nonlinear Dynamics, Cambridge University Press, (2000).